Testing the figure of parabolic reflectors for solar concentrators

J. S. Bodenheimer, N. P. Eisenberg, and Joshua Gur

A novel method for testing the optical quality of large parabolic solar concentrators is presented, based on autocollimation. An optical system continuously scans the reflector along a fixed reference axis. At each position along the axis, the spread function is obtained. Analysis of the location, width, and intensity changes of this function gives quantitative information about the reflector's defects. A figure of merit describing the performance of parabolic trough reflectors is proposed.

I. Introduction

The Shemesh utility system (SUS-I) is a solar energy generation system, which generates industrial process steam by using parabolic trough collectors to focus sunlight onto a selectively coated pipe. The hot liquid is circulated through this pipe and into a heat exchanger which supplies industrial process steam.

The heart of the SUS-I is an array of solar collector modules, each of which is a cylindrical parabolic reflector that tracks the sun's movement (see Fig. 1). The parabolic reflector evaluation facility (PREF) is a testing system, the purpose of which is to evaluate the reflectors at the postproduction stage, in order to measure their performance and determine whether they qualify for installation. Those reflectors found to be substandard are further examined by the system to determine the nature of the defect and its precise location.

The following terminology will be used regarding parabolic trough reflectors (see Fig. 2): The symmetry axis of a 2-D parabola formed by a section of the reflector is termed the parabola axis y. The locus of the sectional parabola focal points in a geometrical ideal system is called the reflector axis z. A section perpendicular to the reflector axis is an $(x\text{-}y)$ section. A section containing the parabola axis and the reflector axis is termed a $(y\text{-}z)$ section. A section perpendicular to the parabola axis is called an $(x\text{-}z)$ section. These definitions will also be used in nonideal systems—although there they are not entirely adequate—as long as ambiguity is avoided.

The specified dimensions of the SUS-I reflector were 33.5-cm focal length, 160-cm aperture, and 400-cm length. Assuming an ideal parabola and illumination by a source of 9×10^{-3}-rad angular extent at infinity, the $(x\text{-}y)$ section of the focal region extends ~8 mm along the parabola axis and 4 mm laterally. The SUS-I reflector specification requires that solar radiation be reflected into a focal region of 3-cm diam or less.

Two modes of operation are required of the PREF:

(a) Semiquantitative evaluation during the development stage of prototype reflectors. The main objectives are to find out whether the construction technique produces a reflector of adequate quality and where gross improvement is required. The time consumed per evaluation is not a major factor in this stage.

(b) Quantitative evaluation of production-line reflectors. The distribution of the reflected radiation should be determined around the focus with at least 0.5-cm resolution.

For those reflectors that are out of tolerance, further evaluation is performed to locate the defective regions. The PREF should be microprocessor-compatible for information evaluation; visual display must be fast and reliable. When the module is constructed from several elements, relative misalignment must be easily detectable.

Various approaches to solar concentrator testing devices published recently were analyzed. It is possible to divide these methods into three main categories: (a) An on-surface point-by-point evaluation.[1,2] A laser beam scans the reflector surface and deviations from the theoretical path are monitored at various points on the reflector. (b) A moiré technique, using moiré fringes

When this work was done all authors were with Jerusalem College of Technology, Electrooptics Department, P.O. Box 16031, Jerusalem, Israel; N. P. Eisenberg is now with Luz International, Ltd., P.O. Box 7929, Jerusalem, Israel.

Received 8 May 1982.

0003-6935/82/244434-05$01.00/0.

© 1982 Optical Society of America.

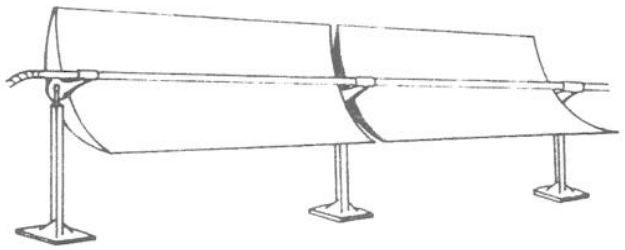

Fig. 1. Schematic of solar collector modules used in SUS-I system.

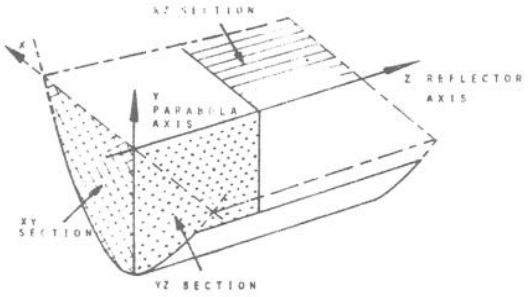

Fig. 2. Illustration of terminology used regarding parabolic trough reflectors.

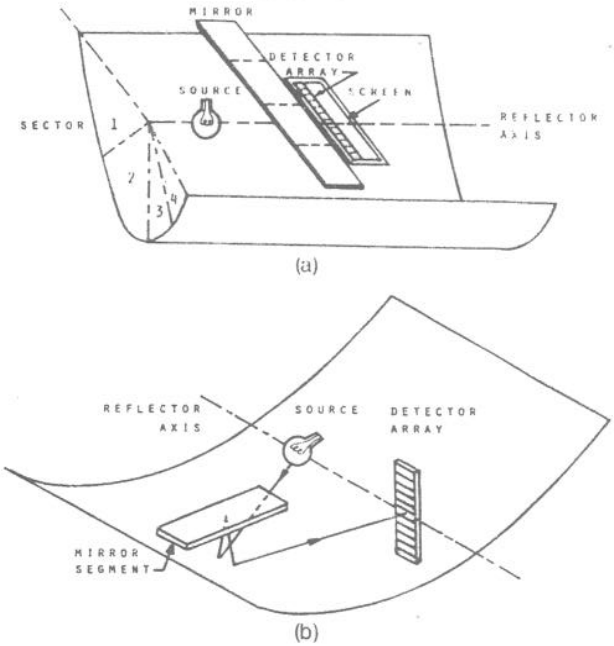

Fig. 3. Schematic representation of the testing method: (a) basic components of the system; (b) retroreflected beam path.

to extract topographical information.[2] (c) Focal point evaluation using a scatterplate.[3]

In addition to the basic requirement of adequate sensitivity consistent with system specifications, a production testing device should possess the following features: fast, with on-line evaluation; convenience of operation; ability to discern between different types of defect; and cost-effectiveness. These requirements led us to a novel approach to the problem of testing parabolic trough reflectors of large dimensions, which is based on autocollimation of a small light source at the focus of the parabola.[4] This method turned out to be convenient enough that, in the preliminary stages of prototype module production, the PREF was actually used as an on-line construction guide to indicate faulty regions of the reflector.

The remainder of this paper describes the testing device as developed for use with SUS-I. In Sec. II the method is discussed in detail. In Sec. III the design of the testing device and alignment of the system are described. Experimental results are given in Sec. IV.

II. Testing Method

The autocollimation method is described in Fig. 3. A light source filament is positioned along the z axis. The radiation emitted by the source is collimated by the parabolic reflector. Part of the collimated beam is intercepted by a plane mirror (referred to as the mirror) and retroreflected onto the reflector, which then images the source at the parabola focus adjacent to the light source as shown in Fig. 3(b). The image and source are symmetrically displaced relative to the mirror, along the z axis.

Examination of the reflected light distribution enables evaluation of the reflector; this is done either by visual inspection on a screen or by a detector array.

The unit consisting of the source, mirror, and image plane can be displaced along the reflector axis for evaluation of different (x-y) sections. To separate between contributions from various regions of the parabola for detailed analysis, the reflector is examined in angular sectors. This is achieved by limiting the mirror aperture, in the present case to one-quarter of the full aperture. Four scans, each corresponding to one of these sectors, enable examination of all parts of the reflector. By comparing broadening and displacement of the image at different positions along the reflector axis, it is possible to identify the various reflector defects described in Sec. IV.A.

The double passing of the light is an inherent feature of autocollimation techniques, leading to the high accuracy of this method. However, in the present method, this feature is slightly modified by the displacement of the retroreflected beam on the reflector as shown in Fig. 3(b). Since the incandescent filament can be considered a line source, the image is essentially the line spread function of the system consisting of reflector–mirror–reflector.

The merit function $f_m(z)$ is defined, at each point z along the reflector axis, as that part of the image flux falling within the limits defined by the collector pipe divided by the total flux reflected by the sector m of the parabola which is examined ($m = 1 \ldots 4$). If the image flux is measured by an array of detectors, $2k + 1$ of which correspond to the pipe diameter, then

$$f_m(z) = \left[\sum_{j}^{+k}{}_{-k} I_{mj}(z)\right]\left[\frac{1}{2\theta_m}\int_{-\theta_m}^{+\theta_m} I_m(\theta,z)\,d\theta\right]^{-1}, \qquad (1)$$

where $I_{mj}(z)$ is the image flux at the jth detector, $\pm\theta_m$ are the angular limits of the mth sector, and

$$\frac{1}{2\theta_m}\int_{-\theta_m}^{+\theta_m} I_m(\theta,z)\,d\theta$$

is the total reflected flux $I_o(m,z)$ for the mth sector.

The reflector figure of merit (FM) is the integrated merit function along the reflector length L and over all four sectors:

$$\mathrm{FM} = \sum_{m=1}^{4}\frac{1}{L}\int_0^L f_m(z)\,dz$$

$$= \sum_{m=1}^{4}\frac{1}{L}\int_0^L \left\{\left[\sum_{j=-k}^{+k} I_{mj}(z)\right]\left[\frac{1}{2\theta_m}\int_{-\theta_m}^{+\theta_m} I_m(\theta,z)\,d\theta\right]^{-1}\right\}dz. \quad (2)$$

Noting that the total reflected flux

$$\frac{1}{2\theta_m}\int_{-\theta_m}^{+\theta_m} I_m(\theta,z)\,d\theta$$

is essentially a constant I_o independent of m and of z, this equation simplifies to

$$\mathrm{FM} = \sum_{m=1}^{4}(I_o L)^{-1}\int_0^L \sum_{j=-k}^{k} I_{mj}(z)\,dz. \quad (3)$$

Thus, the figure of merit is obtained simply by integrating the outputs of $2k + 1$ detectors as they are scanned along the reflector axis, over the four parabola sectors $m = 1 \ldots 4$.

If the reflector FM is within specifications no additional evaluation is necessary. Only when the FM is below a specified value, further processing of the detector array output or visual analysis may be carried out to determine the nature of the defects and their location.

III. Device Design and Alignment

Various approaches to construction of the PREF main frame were considered. In the final design, the reflector is mounted onto the main frame in a fixed position with its aperture vertical as shown in Fig. 4. Thus, the main frame consists of two connected mechanical units. One unit is the reflector mount which defines a reference axis; the second is a mount for the optical system which enables its movement along the axis defined by the first unit. Specifically, the optical system rolls on bearings along two rods which are initially aligned parallel to the reference axis. These 4-m long rods are supported from the ends of the main frame. Additional support is provided by posts placed at suitable intervals.

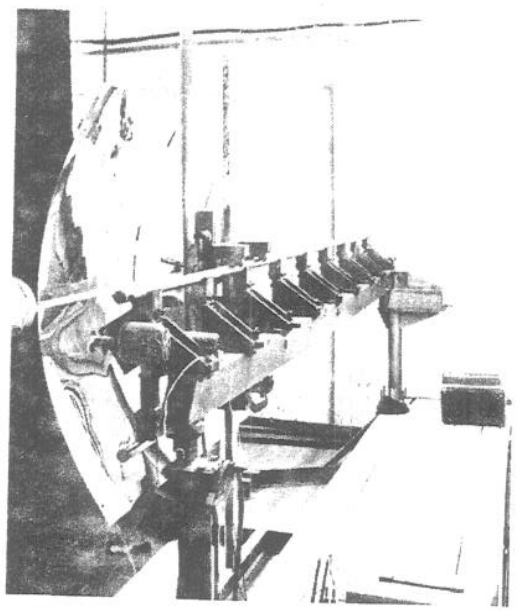

Fig. 4. Parabolic reflector evaluation facility showing reflector mounted in testing position.

The plane mirror is positioned parallel to the $(x\text{-}z)$ plane of the reflector. Its dimensions are 160×3 cm, with the long dimension parallel to the x axis. A mask covering the mirror defines an aperture of 40×2 cm, and this aperture can be set at four locations to mask off different regions of the mirror. For more detailed examination of the reflector, it is possible to reduce the effective aperture.

The source, screen, and detectors can be rotated together between four sector test positions at preset angles around the reflector axis. These orientations are linked to the mirror aperture position, so that for each of the four mirror aperture locations, the source, screen, and detectors face the parabola sector being examined.

The lamp housing is designed to minimize the amount of unwanted radiation traversing the optical system. For visual inspection of the reflected light distribution in the image, a ground glass screen with a scale is provided. The detector system is an array of fifteen photosensitive elements, each measuring 5×5 mm, with minimal spacing. The detector housing is designed to shield the detectors from stray light. Silicon photovoltaic cells operating in the current mode were found to be suitable detector elements.

Initial alignment of the PREF is performed as follows: using a helium–neon laser, an optical axis is defined by passing the beam through two circular apertures at opposite sides of the reflector mount. This serves as the fixed reference axis. The light source filament should be coincident with the optical axis preferably within ± 0.5 mm at all positions along the assembly, which means that the main-frame rods should be parallel to the optical axis within this tolerance. Next, the mirror is angularly aligned in a vertical direction. A misalignment angle θ will cause an image shift of $2\theta l$, where l is the reflector-to-image distance. Therefore, mirror alignment should be maintained within $\pm 0.6 \times 10^{-3}$ rad of the perpendicular when the system is scanned along the rods (i.e., any shift in image position should be due to variations in the reflector, not in the mirror or the filament position). This mirror alignment is achieved by fine adjustment of the rods. Additional mirror alignment is possible by means of spring-loaded screws. Since the mirror is in a vertical position, bending problems are minimal.

Precise angular adjustment is monitored by pointing a second laser beam at one end of the long dimension of the mirror while the system scans along the rods. If the two beams are parallel to each other within 0.5 mm over the length of the rods, this is an extremely useful alignment aid. The laser defining the optical axis remains in position after alignment has been completed and is used for localized reflectance measurements.

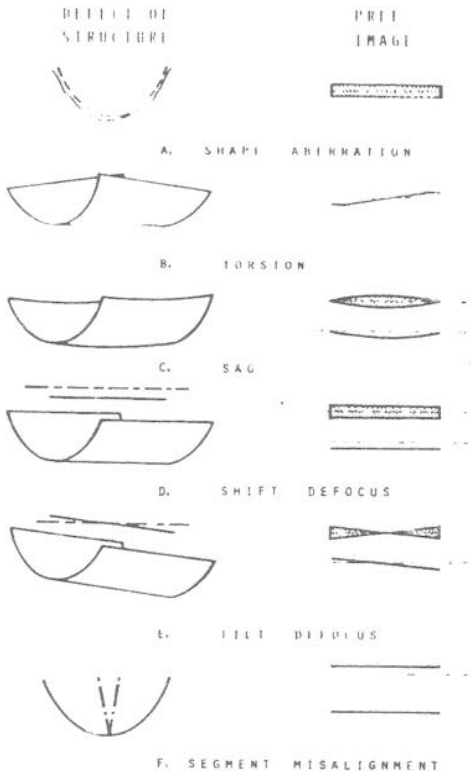

Fig. 5. Primary defects of reflector structure and their characteristic effect on the PREF image.

IV. Results

A. Defect Analysis

Six primary defects of the reflector structure have been defined and their various effects on image shape analyzed. These are briefly described in the following and illustrated in Fig. 5.

(1) Shape aberration in $(x\text{-}y)$ sections caused by imperfect forming of the parabola and resulting in nonuniform broadening of the image.

(2) Torsion between various $(x\text{-}y)$ sections along the z axis caused by structural twisting.

(3) Structural sag in the $(y\text{-}z)$ and $(x\text{-}z)$ sections. Sag in the $(y\text{-}z)$ section causes image bending to appear in sectors $m = 1$, $m = 4$, and image broadening at the scanning center in sectors $m = 2,3$. For $(x\text{-}z)$ sag, bending appears in sectors 2 and 3 and broadening in sectors 1 and 4.

(4) Longitudinal or transverse defocusing due to shift of reflector axis relative to collector pipe axis. The longitudinal (y-axis) component of the shift causes uniform image displacement in scanning the $m = 1,4$ sectors and uniform broadening in sectors 2 and 3. The transverse (x-axis) component causes displacement in sectors 2 and 3 and broadening in sectors 1 and 4.

(5) Longitudinal or transverse defocusing due to tilt of reflector axis relative to collector pipe axis. The longitudinal component in the $(y\text{-}z)$ plane causes angular image displacement evident in sectors 1 and 4. In the sectors 2 and 3, angular broadening occurs. For the transverse component (in the $x\text{-}z$ plane) these effects in the sector pairs are interchanged.

(6) Misalignment between reflector segments. Depending on reflector construction, segment misalignment can take various forms and analysis should be adapted to each particular construction. In general, this defect is characterized by a discontinuous change in image position or width in a scan along the z axis.

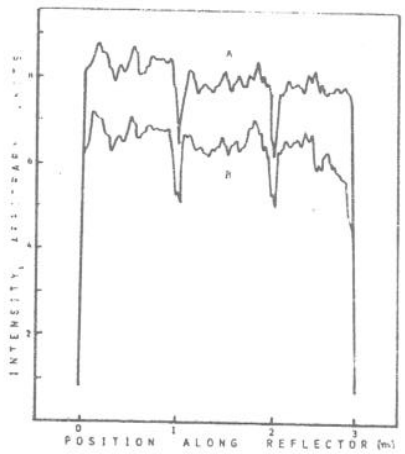

Fig. 6. Typical PREF output showing summation of 15 detector elements in A and 5 detectors in B. Note the decrease in output corresponding to seams between the three reflector panels.

B. Reflector Evaluation

During the construction of prototype reflectors, regions of inferior quality were identified on the reflector. The source of the defect was usually traced to faulty shaping of the reflector sheet. As a result, an improved method of attaching sheets to the structural support was developed. At this stage, visual inspection using the ground glass screen proved extremely effective. At a more advanced stage, reflectors were evaluated quantitatively.

The merit function $f_m(z)$ as defined in Sec. II is obtained by summing the outputs of $2k + 1 = 5$ centrally located detector elements. These cover a width of 2.5 cm, to which the additional broadening due to the angular width of the solar disk is added, to give the effective pipe diameter. For comparison, the outputs of 15 centrally located detector elements are also summed covering a width of 7.5 cm.

The overall figure of merit is obtained by summation of the 5-element trace areas for all 4 sectors. A 70% efficiency is typical for the reflectors tested. A typical result is shown in Fig. 6. The lower trace shows the sum of the 5 central detector outputs as a function of position along the pipe axis for one sector ($m = 3$). Integration of the trace area yields a geometric efficiency of 80% for this sector, which corresponds to a reflector efficiency of 74%. The upper trace gives the sum of 15 detector outputs for the same sector. The integrated trace area corresponds to a reflector efficiency of 90%. Incidentally, the result obtained from 25 elements did not differ significantly from the 15-detector trace (<1% integrated flux).

V. Conclusion

The PREF has proved to be a versatile tool for examination of parabolic trough reflectors, serving two purposes: (A) development stage evaluation of reflector construction concepts, and (B) production-line control of reflector quality.

Its major advantages are:

(1) The figure of merit of a reflector, corresponding to overall reflector efficiency, can be obtained within minutes.

(2) The integrative character of the PREF enables one to follow behavior of large areas of a reflector.

(3) Structural defects can be analyzed by their various effects on the image shape.

(4) Reflector performance is easily evaluated either qualitatively by visual means or quantitatively using a series of detector elements.

The authors wish to thank Joseph Rogozinski for his assistance with the mechanical design of the PREF. A partial description of the method was presented at the OSA 1980 Annual Meeting.

References

1. B. D. Hansche, ISA Trans. **19**, 43 (1980).
2. J. W. Griffin, J. Opt. Soc. Am. **70**, 1630 (1980).
3. K. Masterson, M. Lang, and M. Bohm, J. Opt. Soc. Am. **70**, 1631 (1980).
4. D. Malacara, *Optical Shop Testing* (Wiley, New York, 1978), Appendix 4.

Applied Optics

Of Optics and Opticists

The Managing Editor welcomes news from any source. It should be addressed to P. R. WAKELING, WINC, 1613 Nineteenth Street, N. W., Washington D. C. 20009

Math and music: the deeper links

Edward Rothstein

How two abstract systems shape our understanding of reality is discussed in this article, which originally appeared in the Arts and Leisure Section of *The New York Times* 29 August 1982 and is reprinted here by permission. © 1982 The New York Times Company.

Before setting out to make my way in the music business, I was in training to become a pure mathematician. Such esoteric subjects as Algebraic Topology, Measure Theory and Non-standard Analysis were my preoccupations. I would stay up nights trying to solve knotty mathematical problems, playing with abstract phrases and structures. But at the same time, I would be lured away from these constructions by another activity. With an enthusiasm that could come only when critical faculties are in happy slumber, I would listen to or play a musical composition again and again, imprinting my ear and mind and hands with its logic and sense. Music and math together satisfied a sort of abstract appetite, a desire that was partly intellectual, partly esthetic, partly emotional, partly, even, physical.

I offer these autobiographical facts only because they are not extraordinary among those who have been involved with these fields. Not only did I know other people tempted by both worlds, but, in various ways, music and mathematics have been associated throughout history.

Mathematicians and physicists of all epochs have felt such affinities. Galileo speculated on numerical reasons "why some combinations of tones are more pleasing than others." Euclid wondered about those combinations some 2000 years earlier. The 18th-century mathematician Leonhard Euler wrote a discourse on the relationship of consonance to whole numbers. Johannes Kepler believed the planets' revolutions literally created a "music of the spheres"—a sonic counterpart to his mathematical laws of planetary motion.

Musicians, on the other hand, have invoked mathematics to describe the orderliness of their art. Chopin said, "The fugue is like pure logic in music." Bach, the fugue's most eminent explorer, also had a predilection for its precise relative, the canon, which he often treated as a puzzle.

In this century, mathematical language has pervaded much musical thinking. Schoenberg's "serial" system for manipulating the scale's 12 tones has exercised enormous influence. Other composers have tried to systematize "duration," "timbre" and "volume." Following suit, contemporary musicologists invoke "set theory," "Markov chains" and other mathematical concepts. Journal articles detail attempts to decompose, perform and compose music using computer programs. Iannis Xenakis applies sophisticated mathematical theories in his compositions. Even John Cage, in his search for *luck* of order, uses computer generated random numbers for composing.

This contemporary use of mathematical concepts in music makes it all the more important that their connections be understood. Why, after all, should math and music be connected? Music is an art, mathematics a science. Music poses no problems, mathematics thrives on them. Music has no practical use, mathematics often does. Music is sensuous, mathematics abstract. Analogies may just be vague metaphor or trivial coincidence.

But fundamental musical elements can be analyzed numerically—as the ancient Greeks knew. Pythagoras, to whom fundamental mathematical discoveries are attributed, believed music to be the expression of number in sound. Aristotle said of the Pythagoreans, "They supposed the whole heaven to be a *harmonia* and a number."

continued on page 4440